Title
Nanopriming and AI for Sustainable Agriculture: Boosting Seed Germination and Seedling Growth with Engineered Nanomaterials, and Smart Monitoring through Deep Learning

Permalink
https://escholarship.org/uc/item/1682r4r5

Journal
ACS Applied Nano Materials, 7(8)

ISSN
2574-0970

Authors
Yeasmin, Samia
Dipto, Asif Rahman
Zakir, Atique B
et al.

Publication Date
2024-04-26

DOI
10.1021/acsanm.4c00109

ACS APPLIED NANO MATERIALS

www.acsanm.org Article

Nanopriming and AI for Sustainable Agriculture: Boosting Seed Germination and Seedling Growth with Engineered Nanomaterials, and Smart Monitoring through Deep Learning

Samia Yeasmin, Asif Rahman Dipto, Atique B. Zakir, Saumik Dey Shovan, Md Amran Hossen Suvo, Mahabub Alam Bhuiyan, Md. Nurul Amin, Taslim Ur Rashid, Sharnali Islam, and Ahsan Habib*

Cite This: https://doi.org/10.1021/acsanm.4c00109 Read Online

ACCESS | Metrics & More | Article Recommendations | Supporting Information

ABSTRACT: Sustainable agriculture, essential for global food security, calls for innovative methods to improve crop yields and conserve resources. Nanopriming, utilizing nanoparticles to enhance seed germination and growth, builds preresistance to diseases and reduces dependence on pesticides and fertilizers. Here, we address two major challenges in the field: effects of varying nanoparticle sizes on seed nutrient enhancement and the lack of efficient, automated systems for germination monitoring. Focusing on zinc oxide (ZnO) nanoparticles, we synthesize them using hydrothermal and solvothermal methods. Our experiments on bitter gourd (*Momordica charantia*) and red amaranth (*Amaranthus gangeticus*) show that nanopriming with these particles, especially those smaller than 30 nm, significantly improves seed germination and seedling growth. Specifically, we observe up to a 23% increase in germination and a 40% rise in shoot length for bitter gourd and a 43% increase in germination with a 20% boost in shoot length for red amaranth. Nanopriming at a concentration of 150 mg/L significantly enhances bitter gourd plant growth, with a notable 90% increase in height and 74% increase in leaf count compared to hydroprimed plants, showcasing the positive impact on fresh biomass production. For field-level monitoring, we propose a sophisticated smart monitoring system incorporating a custom-designed two-axis CNC machine with a single-board computer and high-resolution camera to redefine seed germination and growth assessment.

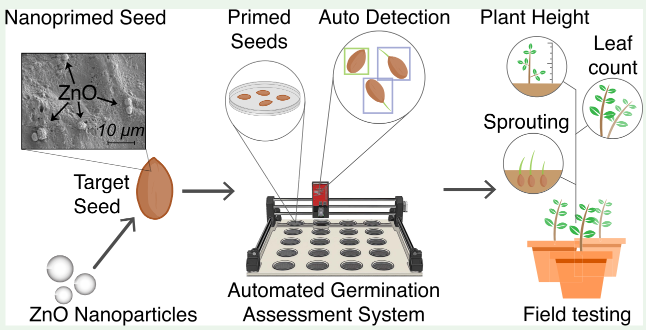

KEYWORDS: *nanopriming, artificial intelligence, sustainable agriculture, seed germination, seedling growth, engineered nanomaterials, smart monitoring, deep learning*

■ INTRODUCTION

In the 21st century, agriculture, a cornerstone of human sustenance and global prosperity, is facing a formidable challenge.[1] Balancing the urgent imperative to increase food production for our growing global population with the critical need to protect our environment and natural resources is a defining concern.[2] It is in this context that sustainable agriculture emerges as our guiding star, steering us toward a more resilient and food-secure future.[3,4] Sustainable agriculture fundamentally seeks to maximize crop yields while minimizing the utilization of resources and environmental impact.[5] Within this ambitious framework, we encounter numerous challenges, including land conversion, water scarcity, and the ecological consequences of agrochemical use. These challenges necessitate innovative approaches that can enhance agricultural productivity while simultaneously mitigating its resource intensity and ecological consequences.[6,7]

In recent years, engineered nanomaterials (ENMs) have arisen as a potent force of innovation, poised to revolutionize agriculture.[8−11] The unique attributes of ENMs, particularly their ability to penetrate plant tissues through mechanisms, such as stomatal penetration due to their nanoscale dimensions, are notable.[12] Additionally, ENMs exhibit high adsorption, a large number of reactive sites, elevated catalytic activity, and high chemical stability.[13] These characteristics render ENMs a promising strategy for enhancing plant growth and productivity.[14,15] Moreover, they have the potential to improve crop stress tolerance, enhance plants' nutritional absorption,[16] and provide protection against both biotic and abiotic stress factors.[17−20]

Received: January 6, 2024
Revised: March 15, 2024
Accepted: March 22, 2024

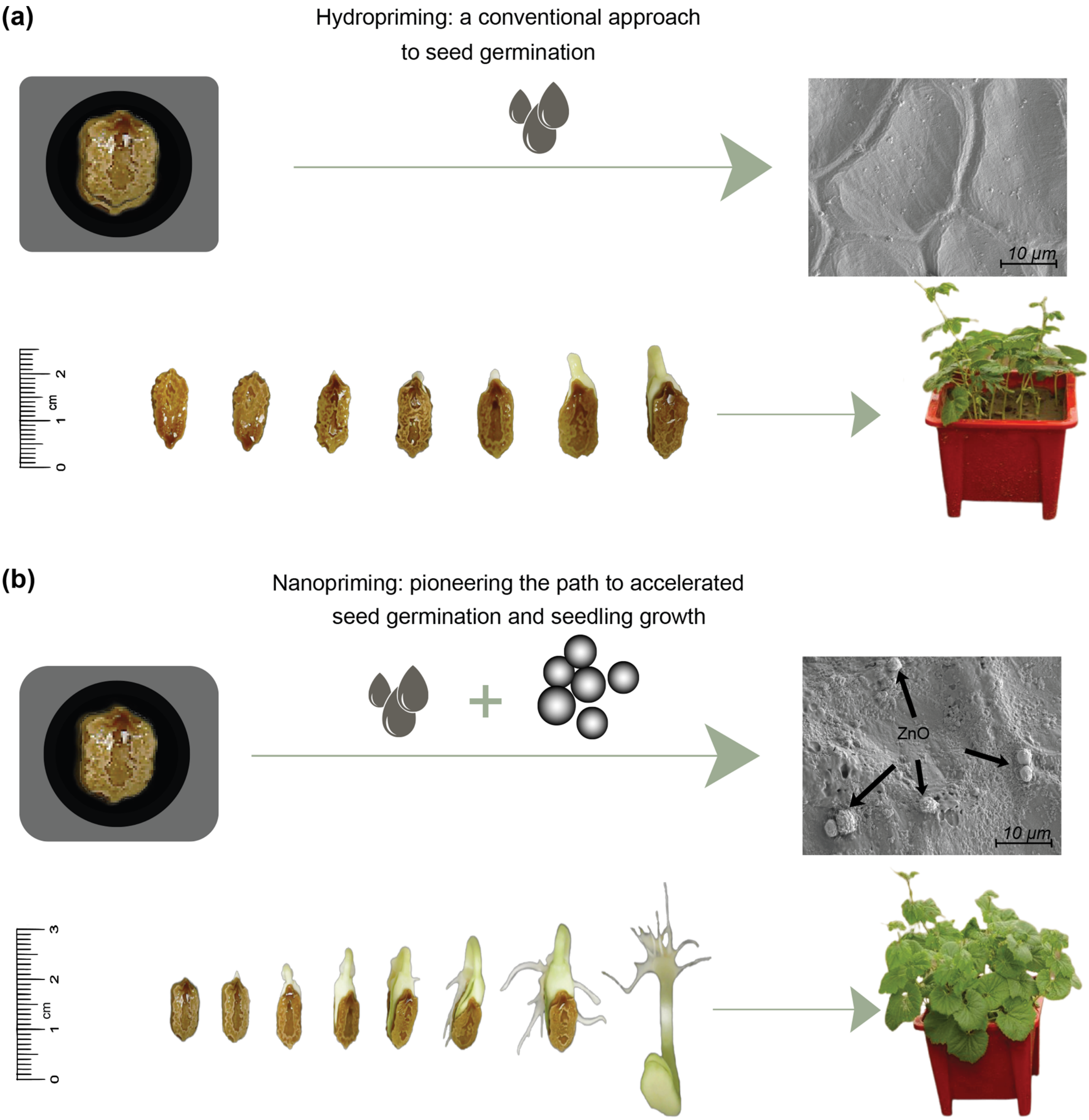

Figure 1. Impact of nanopriming on seed germination and seedling growth. (a) Top Panel: SEM image of cross-section of bitter gourd seeds after conventional hydropriming for 24 h, demonstrating limited structural changes. Bottom Panel: Corresponding seed germination and seedling growth data. (b) Top Panel: SEM image of the cross-section of bitter gourd seeds after nanopriming with Type-3 ZnO NPs at 150 mg/L, revealing the presence of aggregated ZnO nanoparticles within the seeds. Bottom Panel: corresponding seed germination and seedling growth data. Our results highlight the substantial enhancement in seed germination and seedling growth achieved through nanopriming compared with the hydropriming control.

ENMs hold great potential in various agricultural applications, including seed priming[21] and foliar treatments.[22] Seed priming, an integral part of agricultural practices, involves pretreating seeds with specific compounds, either natural or synthetic, under controlled conditions to enhance their germination potential and subsequent crop yield. This technique initiates metabolic activities associated with germination without the emergence of the radicle. Priming solutions commonly used are hydropriming (using water),[23] osmopriming (involving polyethylene glycol and inorganic salts),[24] hormonal priming,[25] and nutrient priming.[26] However, the effectiveness of these priming solutions can vary depending on the properties of the solution and the specific requirements of different crop species.[27] Integrating ENMs into seed priming processes offers a novel approach to enhance crop productivity and quality potential, providing valuable solutions for sustainable agriculture.

https://doi.org/10.1021/acsanm.4c00109
ACS Appl. Nano Mater. XXXX, XXX, XXX−XXX

Recently, various metal-based ENMs, including nanoparticles (NPs) like ZnO NPs,[28] Fe NPs,[29] Ag NPs,[30] and Ag/ZnO NPs[31] have demonstrated potential in enhancing seed germination rates (SGR) even under stressful conditions. ZnO NPs, in particular, have emerged as highly applicable ENMs in agriculture.[32,33] Zinc, a vital micronutrient, plays a crucial role in supporting optimal plant growth by facilitating processes, such as synthesis of photosynthetic pigments, cell division, and overall plant development.[34] ZnO NPs have been found to positively impact shoot growth rate, plant growth, and yield, even under stress conditions.[35] The significance of zinc is well documented across various studies, as it actively enhances protein metabolism, and enzyme function, that are essential for plant health.[36] Furthermore, the application of ZnO NPs has been shown to significantly improve the enzymatic activity of superoxide dismutase (SOD), catalase (CAT), and glutathione reductase (GR) under metal stress, further highlighting the defensive role of NPs in adverse environments.[37]

However, despite advances in ENM research, significant knowledge gaps remain. Questions about the influence of varying nanoparticle sizes on seed nutrient enhancement through priming and the absence of efficient, automated systems for monitoring germination and seedling growth constitute crucial gaps in our current understanding. Most studies to date have predominantly focused on nanomaterials with fixed crystalline sizes, overlooking the potential influence of varying nanoparticle sizes on the physiochemical properties of these materials.[38,39] Exploring different nanoparticle sizes holds promise for optimizing nanomaterial synthesis for more effective applications. Additionally, achieving the necessary efficacy and robustness required for real-world field applications has remained a challenge.

In light of these challenges, this study aims to bridge critical knowledge gaps. We investigate the influence of varying sizes of ZnO nanoparticles on seed nutrient enhancement through priming with the aim of optimizing plant growth and yield. Additionally, we introduce an automated system designed for precise germination detection under field conditions, significantly expediting the evaluation of seed germination experiments. Our findings demonstrate the substantial potential of ZnO nanoparticles, particularly at a concentration of 150 mg/L, in significantly improving both seed germination and seedling growth compared to hydropriming controls (Figure 1). For red amaranth, this treatment resulted in an impressive 43% increase in germination and a notable 20% boost in shoot length, while bitter gourd exhibited even more remarkable outcomes with a 23% increase in germination and an extraordinary 40% stimulation in shoot length. Furthermore, the critical role of nanoparticle size is highlighted, with smaller nanoparticles surpassing their counterparts in efficacy. For field-level monitoring and assessment, we present an automated, camera-equipped two-axis CNC machine. This setup not only streamlines the process of monitoring and assessing crop growth but also accelerates research in agricultural technology by providing precise and efficient data collection. Our study underscores the substantial potential of ENM nanoparticles in enhancing seed germination, seedling growth, and crop yield, while also demonstrating the practicality of translating these findings into real-world agricultural contexts through advanced technologies like CNN-based automation.

■ MATERIALS AND METHODS

Synthesis of ZnO Nanoparticles. *Materials.* The precursor materials used in this study included zinc acetate dihydrate ($Zn(CH_3COO)_2.2H_2O$) and zinc nitrate hexahydrate ($Zn(NO_3)_2.6H_2O$) for zinc oxide nanopowder synthesis. Sodium hydroxide (NaOH) was used as a coprecipitant, while DI water and ethanol (C_2H_5OH) were used as solvents. All chemicals and reagents were of analytical grade and utilized as received without additional purification.

Hydrothermal Method. In the hydrothermal method, 3.357 g of zinc acetate dihydrate ($Zn(CH_3COO)_2.2H_2O$) and 4.0 g of sodium hydroxide (NaOH) were separately dissolved in 30 mL of DI water with constant stirring. The NaOH solution was then added dropwise to the zinc acetate dihydrate solution under vigorous stirring at room temperature, resulting in the formation of transparent white solutions. The mixture was moved to a Teflon-lined autoclave and positioned within an oven set at 120 °C for a duration of 12 h. Afterward, the resulting precipitate was centrifuged and washed 7−8 times with DI water and 3 times with ethanol. Each wash cycle involved centrifugation at 5000 rpm for 10 min. The obtained nanosized ZnO precipitate was dried at 60 °C in a universal oven for 6 h, ground into a powder, and then calcined in a muffle furnace for 3 h, resulting in ZnO nanoparticles that we termed Type-2 ZnO NP. The same procedure was repeated, replacing zinc acetate dihydrate with zinc nitrate hexahydrate ($Zn(NO_3)_2.6H_2O$) to synthesize ZnO nanoparticles (named Type-1).

Solvothermal Method. In the solvothermal method, 1.48 g of zinc acetate dihydrate ($Zn(CH_3COO)_2.2H_2O$) was dissolved in 63 mL of absolute ethanol while constant stirring was maintained at 60 °C. Concurrently, 0.54 g of NaOH was dissolved in 33 mL of absolute ethanol under the same conditions. Once both solutions were fully dissolved, the NaOH solution was gradually added dropwise to the zinc acetate dihydrate solution at 60 °C with vigorous stirring. The resultant mixture was allowed to react for a duration of 3 h, leading to the formation of a white precipitate comprising ZnO nanoparticles (named Type-3). The precipitate was collected using centrifugation (10000 rpm, 8 min, 4 cycles), subjected to rinsing by DI water and ethanol, and then dried at 60 °C for 12 h.

Characterization of ZnO NPs. The synthesized samples underwent comprehensive characterization using various analytical techniques. X-ray diffraction (XRD) patterns were obtained using a high-temperature X-ray diffractometer (model: PW 3040-X'Pert PRO Philips) equipped with a temperature attachment capable of reaching up to 1600 °C. The XRD analysis employed Cu K_α radiation (λ = 0.15418 nm) over a range spanning from 10 to 80°. For the examination of sample morphology, field-emission scanning electron microscopy (FESEM) was employed, utilizing the "high-resolution FESEM from the ZEISS Sigma Family." Fourier transform infrared (FTIR) spectra were collected across the wavenumber range of 4000−400 cm^{-1} using an FTIR spectroscopy system, specifically the "IR prestige-21, SHIMADZU." Furthermore, UV−vis diffuse absorbance measurements were conducted using a Shimadzu UV-2600i UV−vis-NIR spectrometer, covering wavelengths ranging from 200 to 800 nm. The hydrodynamic size of the sample was estimated from dynamic light scattering (DLS) measurements.

Seed Selection. The thick seed coat often prevents germination by physically restricting embryo growth, leading to poor or delayed seed germination.[40] To depict the influence of ZnO nanopriming across a range of seed types, we specifically selected two plant species: bitter gourd (*Momordica charantia*) and red amaranth (*Amaranthus gangeticus*). Bitter gourd, a member of the *Cucurbitaceae* family is characterized by a thicker seed coat.[40] Red amaranth, from the *Amaranthaceae* family, is distinguished by its thinner seed coat.[41] Seeds of both species, each with an 80% germination rate, were obtained as certified seeds from Bangladesh Agricultural Development Corporation (BADC). Notably, they exhibit low dormancy levels, rapid germination, and efficient seedling development, making them highly suitable for laboratory experiments.

https://doi.org/10.1021/acsanm.4c00109
ACS Appl. Nano Mater. XXXX, XXX, XXX−XXX

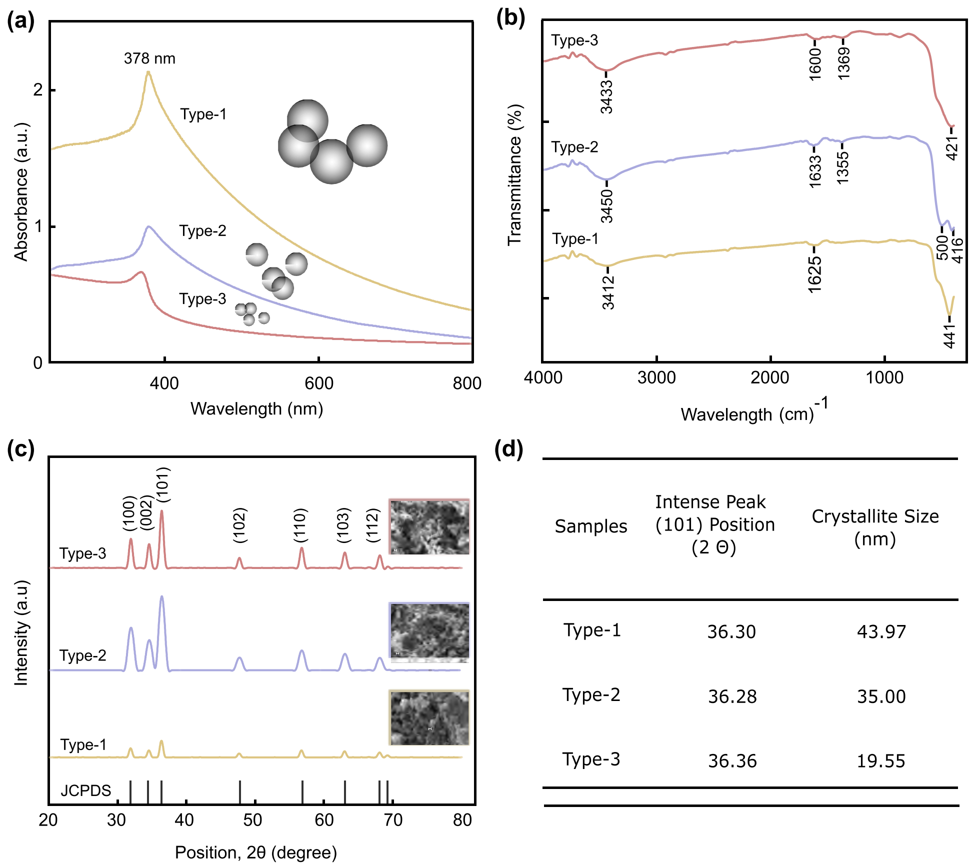

Samples	Intense Peak (101) Position (2 Θ)	Crystallite Size (nm)
Type-1	36.30	43.97
Type-2	36.28	35.00
Type-3	36.36	19.55

Figure 2. Characterization studies of synthesized ZnO NPs: UV−vis absorbance, FTIR spectra, and X-ray diffraction. (a) UV−vis absorbance spectra of the prepared ZnO NPs. (b) FTIR Spectra of synthesized Type-1, Type-2, and Type-3 ZnO NPs revealing its functional groups. (c) X-ray diffraction spectra of synthesized Type-1, Type-2, and Type-3 ZnO NPs. (d) Estimated crystallographic parameters from X-ray diffraction studies.

Preparation of ZnO Nanopriming Solution and Seed Priming. ZnO nanoparticle solutions were prepared at various concentrations (20, 40, 60, 100, 150, and 200 mg/L) by dispersing the nanoparticles in deionized (DI) water and subjecting the solution to 30 min of ultrasonication. For the hydropriming control, only DI water was used. Healthy seeds of bitter gourd (*Momordica charantia*) and red amaranth (*Amaranthus gangeticus*) were chosen for the priming treatment. In the seed priming process, seeds were submerged in the priming solution for a specified duration. Subsequently, they were air-dried at room temperature before being used for further experiments. Conversely, seeds immersed in DI water were designated as the hydropriming (control) group.

Internalization Studies of Zn Content in Primed Seeds. *FESEM Imaging of Seed Surfaces and Quantitative Analysis of Zn Uptake by Seeds.* The dried seeds were affixed to stubs using conductive double-sided carbon tape and then coated with a thin layer of gold before SEM imaging. The energy-dispersive X-ray spectroscopy (EDX) technique was employed to confirm the elemental weight percentage in bitter gourd seeds and to ascertain the relative proportions of the elements in various seed samples.

Quantification of Zn Content in ZnO Nanoparticle-Primed Seeds Using Atomic Absorption Spectroscopy. To determine the zinc content in the primed seeds, atomic absorption spectroscopy (AAS) was employed. Initially, both the hydroprimed and nanoprimed seeds were washed and then dried for 2 days at 65 °C. Following this, dried seeds were ground to pass through a 60 mesh screen. Subsequently, the dry material was weighed in a high-form crucible and placed in a muffle furnace for 3 h at 800 °C. After cooling, it was moistened with a few drops of distilled water, and 10 mL of diluted (1:1) HNO_3 (density 1.41 g/mL) was cautiously added. The solution was filtered, transferred to a volumetric flask, and diluted with water up to 25 mL. The resulting aqueous digest was directly analyzed using a Shimadzu AA-7000 atomic absorption spectrophotometer to determine the zinc concentration.

Germination Assay and Growth Measurement. *Germination Assay of Red Amaranth.* The germination assessment of red amaranth seeds was carried out using the International Seed Testing Association-approved paper towel technique with each type of ZnO NP tested separately. The procedure involved placing sterile tissue paper on a plastic Petri dish (90 × 15 mm). The tissue was then moistened with 15 mL of ZnO NP solutions of varying concentrations for nanopriming, while DI water was used for the control group. In each dish, 25 seeds of uniform size were placed, and this entire experiment was replicated three times for each type of ZnO NPs. The seeds were then kept in the dark for germination at 28 ± 2 °C. Germination was determined by observing the emergence of the radicle protrusion. This observation was recorded at 24 h intervals for a period of 10 days. To prevent drying, 5 mL of distilled water was added to each Petri dish on alternate days. The daily count of germinated seeds was carried out, and the shoot length of the germinated seedlings was measured using a microscope.

Germination Assay of Bitter Gourd. Similar germination tests were performed on both primed and unprimed bitter gourd seeds. However, in this case, only DI water was used to moisten the paper towel, while the remaining steps of the process remained unchanged.

Data Processing. Seeds were placed on moist tissue paper in Petri dishes. A digital microscope (YIERYI 50X-500X Digital Microscope) captured detailed close-up photos of the seeds. Seed images were taken daily for 10 days. To achieve accurate detection and classification of seed germination states and growth measurements, microscope images underwent data processing using the YOLOv5 convolutional neural network (CNN) model. Initially, images were uploaded to Roboflow (https://roboflow.com) for labeling seeds with their germination states, distinguishing between germinated and

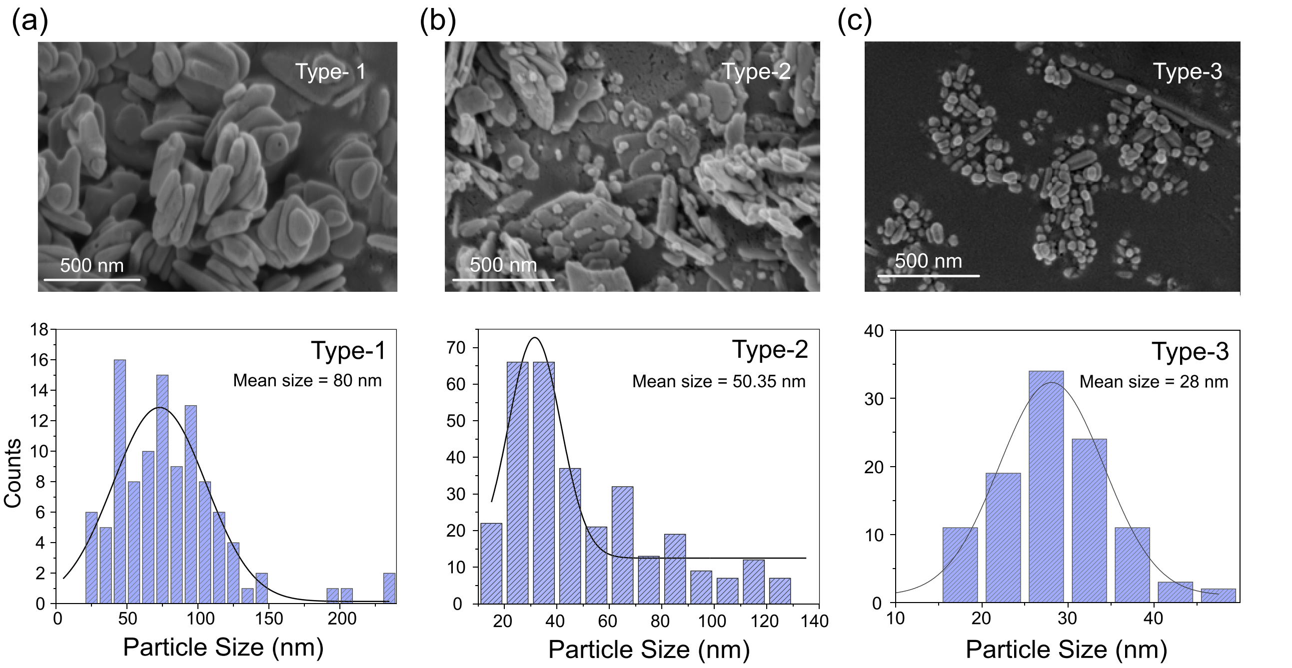

Figure 3. FESEM images and particle size distribution of ZnO NPs. (a) Top Panel, FESEM image; Bottom Panel, particle size distribution for Type-1 ZnO NPs. (b) Top Panel, FESEM image; Bottom Panel, particle size distribution for Type-2 ZnO NPs. (c) Top Panel, FESEM image; Bottom Panel, particle size distribution for Type-3 ZnO NPs.

nongerminated seeds using polygons for precise accuracy. The annotated data were randomly divided into a 70% training set, a 20% validation set, and a 10% testing set. The mean average precision (mAP) after 100 epochs reached 93.87%.

Field Study. For the field test, a total of seven beds, each measuring 8 × 8 in., were designated. Six of these beds were allocated for ZnO-treated seeds, primed with various concentrations (20, 40, 60, 100, 150, and 200 mg/L) of ZnO NPs, and one bed served as a control for hydroprimed seeds. Both ZnO-treated and hydroprimed seeds were directly sown in plastic pots, with each pot containing 30 seeds. The pots were filled with air-dried and well mixed field soil without the addition of any fertilizers. Prior to conducting growth analysis, the nutrient contents of the soil utilized in the pots were assessed using EDX (Table S3). Furthermore, the Zn content of the soil was determined using AAS (see Supplementary Text 5). Seeds were sown uniformly in each pot. Pots were placed in a screen house under natural conditions with temperature regime of 36/25 °C, relative humidity of 65 ± 10%, and 14/10 h light/dark photoperiod. They were uniformly irrigated with distilled water (100 mL) as per the requirement to avoid a water deficit. Seed emergence was counted daily, and Table S6 illustrates the number of plants in each bed. Plant height and leaf count measurements were conducted regularly to evaluate the progress and health of the plants. Plant height was recorded by measuring the length of five randomly selected plants from each bed using measuring tape. The number of leaves per bed was determined by averaging the count of leaves from five randomly selected plants.[42]

Statistical Analysis. All experiments were conducted in triplicate. One-way analysis of variance (ANOVA) was performed using IBM SPSS version 27 Software. Data are presented as mean ± standard error of mean (SEM) (SEM = $\frac{SD}{\sqrt{n}}$, where SD is the sample standard deviation and n is the sample size). Significant differences were tested, and means were compared using two-tailed independent samples Student's t test. Data visualization and graph generation were carried out using the Origin 2021 software.

Cytotoxicity Studies of ZnO Nanoparticles. To assess the cytotoxic effects of ZnO nanoparticles, we utilized two cell lines: HeLa, a human cervical carcinoma cell line, and Vero, a kidney epithelial cell line derived from an African green monkey. Both cell lines were cultured in Dulbecco's Modified Eagle's Medium (DMEM) supplemented with a mixture of 1% penicillin-streptomycin (1:1 ratio), 0.2% gentamicin, and 10% fetal bovine serum (FBS). The cell cultures were maintained in a humidified atmosphere comprising 5% CO_2 and 95% air at 37 °C.

For the cytotoxicity assessment, HeLa cells (2×10^4 cells per 100 μL) and Vero cells (1.5×10^4 cells per 100 μL) were seeded onto 96-well plates and incubated overnight at 37 °C under a 5% CO_2 atmosphere. Following the overnight incubation, the culture medium in the wells was replaced with fresh medium containing 25 μL of a filtered solution of ZnO nanoparticles at a concentration of 150 mg/L. The cells were then incubated for an additional 48 h. Subsequently, cytotoxicity was assessed by microscopic observation using an inverted light microscope. Duplicate wells were utilized for each type of ZnO nanoparticle, and cells incubated without nanoparticles served as the control group for comparison.

■ RESULTS AND DISCUSSION

ZnO Nanoparticle Synthesis and Characterization. Seed preconditioning with ZnO nanoparticles significantly enhances seed germination and supports robust seedling growth and plant development.[43] Key to this process are two critical factors: the crystallite size of the nanoparticles and their concentration. To investigate these aspects, we synthesize ZnO nanoparticles in three distinct sizes using hydrothermal and solvothermal methods. We vary the zinc precursors to actively alter the nanoparticle dimensions. Following this, we characterize the nanoparticles thoroughly. This step is crucial for ensuring the reproducibility of the nanopriming process and understanding its physical and chemical properties.

We employ UV−visible spectroscopy to confirm the formation of ZnO NPs (Figure 2a and Supplementary Text 1). The spectra exhibit a distinct absorption band near ∼375 nm, characteristic of surface plasmon resonance. This confirms the successful synthesis of ZnO NPs in all three samples. This observation is consistent with Al-Asady et al.'s findings.[44] Additionally, the absence of extra peaks in the absorption

https://doi.org/10.1021/acsanm.4c00109
ACS Appl. Nano Mater. XXXX, XXX, XXX−XXX

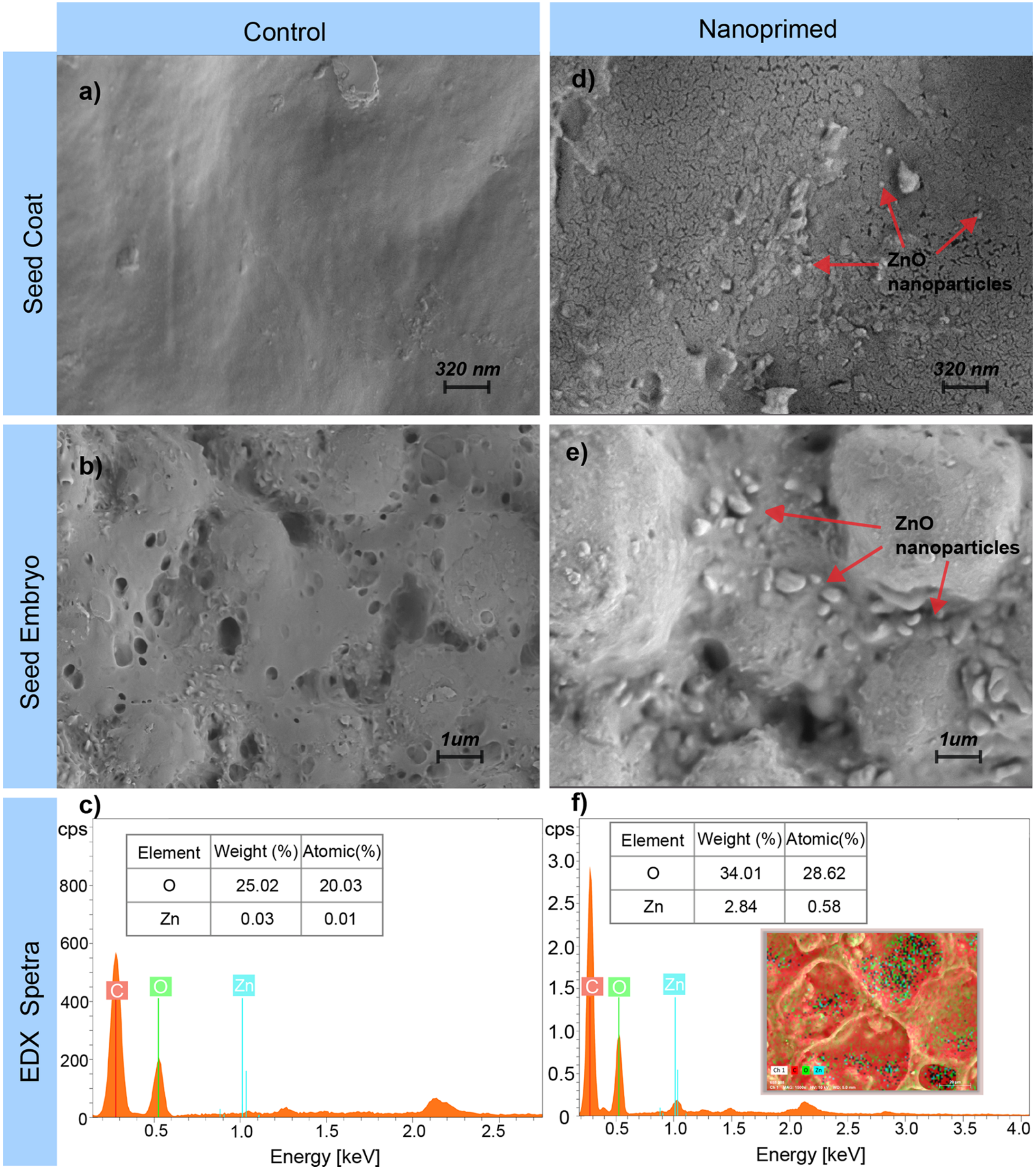

Figure 4. FESEM images of bitter gourd seed surfaces and embryos. (a and b) control (hydroprimed) seeds, (c) EDX spectrum of control seed, (d and e) ZnO NP-treated seeds, and (f) EDX spectrum of ZnO NP-treated seed (inset shows the EDX mapping of nanoprimed seed embryos.

spectra further supports the successful synthesis of a pure ZnO powder. Furthermore, we analyze these spectra using Tauc plots to estimate the bandgap values of the different ZnO NP samples (Figure S1). The energy band gap of ZnO nanoparticles exhibits size-dependent behavior, wherein it decreases with an increase in crystallite size. This trend is attributed to the quantum confinement effect, as discussed in the study by Agarwal et al.[45] This trend is apparent in the bandgap values: 2.82 eV for Type-1, 2.88 eV for Type-2, and 3.18 eV for Type-3 samples, as determined by our UV−vis findings. These variations hint at differences in crystallite sizes among the types, which we will further substantiate in our XRD analysis.

Continuing our analysis, we employ FTIR spectroscopy to identify the functional groups in ZnO NPs (see Figure 2b). Notably, peaks at 498.25 cm^{-1} signify Zn−O stretching vibrations, aligning with previous research[46] and reinforcing the robustness of our ZnO NP synthesis process. In addition, we do XRD analysis (Figure 2c) to examine the phase identity, crystalline nature, and purity of the synthesized NPs. It reveals distinctive diffraction peaks indicative of a crystalline wurtzite structure (JCPDS 00−036−1451) within space group 186: P63mc, with no impurities.[47] The broadness of the XRD peaks indicates nanoscale ZnO particles. Using Debye−Scherrer's equation, we estimate the average nanocrystalline size of the synthesized ZnO NPs to be approximately 43, 35, and 19 nm for Type-1, Type-2, and Type-3 samples, respectively, along with several other pertinent crystallographic parameters derived from the XRD data (Figure 2d, Supplementary Text 3, Table S1).

We employ field emission scanning electron microscopy (FESEM) to investigate the morphology and size of ZnO nanoparticles. Figure 3 displays FESEM images of the synthesized Type-1, Type-2, and Type-3 ZnO nanoparticles

https://doi.org/10.1021/acsanm.4c00109
ACS Appl. Nano Mater. XXXX, XXX, XXX−XXX

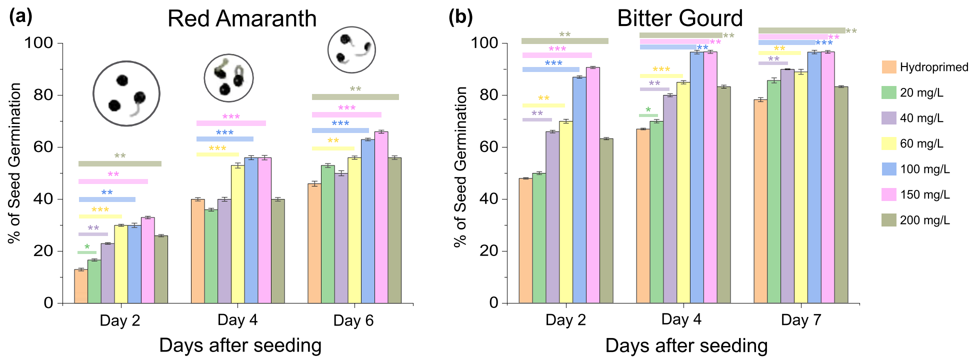

Figure 5. Effect of NP seed priming on the dynamic of seed germination under different concentrations of Type-1 ZnO NPs. (a) red amaranth and (b) bitter gourd. Data are presented as means of three replicates containing 25 seeds each ± standard error of means. Statistical differences between the mean of treatments (various concentrations of ZnO NP priming solutions) compared to the control are denoted by (*, $p < 0.05$; **, $p < 0.01$; ***, $p < 0.001$) according to an Independent sample Student's t test.

and their corresponding size distributions. We select a random sample of at least 100 particles from each FESEM image to construct frequency tables and histograms for the particle size distribution. Subsequently, we convert these distributions to normalized forms, as illustrated by the solid lines in the graphs of Figure 3. The average particle sizes for Type-1, Type-2, and Type-3 are 80, 50, and 28 nm, respectively. The nanoparticle sizes obtained through FESEM and those calculated from XRD data using the Scherrer equation show variations, but they consistently demonstrate the same trend: Type-1 > Type-2 > Type-3.

Complementing the FESEM findings, we analyze the hydrodynamic size of ZnO nanoparticles in DI water using DLS to gain insight into their colloidal characteristics. Additionally, zeta potential measurement is employed to assess the surface charge of the nanoparticles. Our DLS data, presented in Supplementary Text 4, Table S2, and Figure S2, aligns with the findings of previous studies.[28,46] The measured hydrodynamic diameters- 365 nm for Type-1, 301 nm for Type-2, and 203 nm for Type-3 in DI water are notably larger than the sizes observed via FESEM. This discrepancy suggests the formation of agglomerates rather than aggregates, as the FESEM images (Figure 3) show nanoparticles with clear grain boundaries.[48] These larger hydrodynamic sizes likely stem from agglomerates, which are clusters of primary particles joined by weak van der Waals forces in the aqueous dispersion. Furthermore, we record average zeta potentials of 12.8, 16.5, and 12.7 mV for Type-1, Type-2, and Type-3 nanoparticles, respectively, consistent with reported values[28]

Assessment of ZnO Nanoparticle Absorption in Primed Seeds. The success of nanopriming depends on the absorption of ZnO nanoparticles into the seed via a seed coat. We utilize FESEM-EDX and AAS to explore the absorption of ZnO nanoparticles within bitter gourd seeds (Figure 4). In Figure 4a, the FESEM image illustrates the smooth surface of the control seeds. The accompanying EDX graph (Figure 4c) indicates the presence of carbon (C) and oxygen (O) content. Zn is detected in negligibly low weight percentage (<0.05%). In contrast, nanoscale ZnO-treated bitter gourd seeds exhibit the absorption of nanoparticles on the seed surface (Figure 4d) and their penetration into the seed embryo (Figure 4e). This observation is confirmed by EDX analysis, which confirms the presence of zinc (Zn), oxygen (O), and carbon (C) (inset of Figure 4f), indicating the successful absorption of nanoscale ZnO by the seeds.[49,50]

Additionally, we employ AAS which is a widely employed technique for the quantitative detection of metal ions[51,52] to measure the uptake of zinc content by ZnO nanoparticle-treated bitter gourd seeds. The zinc content in the hydroprimed seeds (control) is approximately 3.98 ppm (parts per million), while it is 10.48 ppm in the nanoprimed seeds. The results indicate that the zinc content in nanoprimed seeds is approximately 2.6 times higher compared to that of the hydroprimed seeds (control). Based on the AAS results, coupled with EDX measurements, it can be inferred that the ZnO NP-treated seeds exhibit a higher zinc uptake.[49,50]

Impact of Nanopriming on Germination and Seedling Growth Traits. ZnO NP priming significantly accelerates early germination and increases germination percentage compared to unprimed and hydroprimed seeds,[53] attributed to enhanced nanoparticle penetration, controlled oxidative stress, nutrient supply, and increased enzyme activity. Our experiments with red amaranth and bitter gourd seeds show significant improvements ($p < 0.05$) compared to the control in both early germination and final germination (FG%) with all three ZnO NP types at various concentrations, indicating a concentration-dependent impact that peaks at 150 mg/L ($p < 0.001$) (Figures 5 and S4). Specifically, for Type-1 NPs, enhancement is evident from the second day postnanopriming (Figure 5). On the sixth day, the FG% for red amaranth ranges from 50% at 40 mg/L to 56% at 200 mg/L of ZnO NP concentrations, with a notable peak observed at 150 mg/L, reaching 66%. Consequently, the FG% of the nanoprimed seeds surpasses that of the hydroprimed seeds, which measure 46% ($p < 0.05$). Similarly, nanoprimed bitter gourd seeds outpace hydroprimed seeds on day 2 ($p < 0.01$) (Figure 5b). Type-2 and Type-3 ZnO NPs consistently showed similar results (Figure S4).

Our experiments confirm that nanoprimed seeds display a faster FG%, consistent with prior research,[30,53,54] supporting ZnO NPs' effectiveness in enhancing seed germination. This improvement can be attributed to several factors. First, priming treatments enhance seed water absorption due to the creation of nanopores on the seed surface.[55] This increased water uptake further stimulates the activities of dehydrogenase, a key enzyme in cellular respiration, in the seedling roots of nanopriming treatments, leading to improved seed germination.[30] Additionally, Zn^{2+} induces a range of biochemical changes in seeds necessary to initiate the germination process,

https://doi.org/10.1021/acsanm.4c00109
ACS Appl. Nano Mater. XXXX, XXX, XXX−XXX

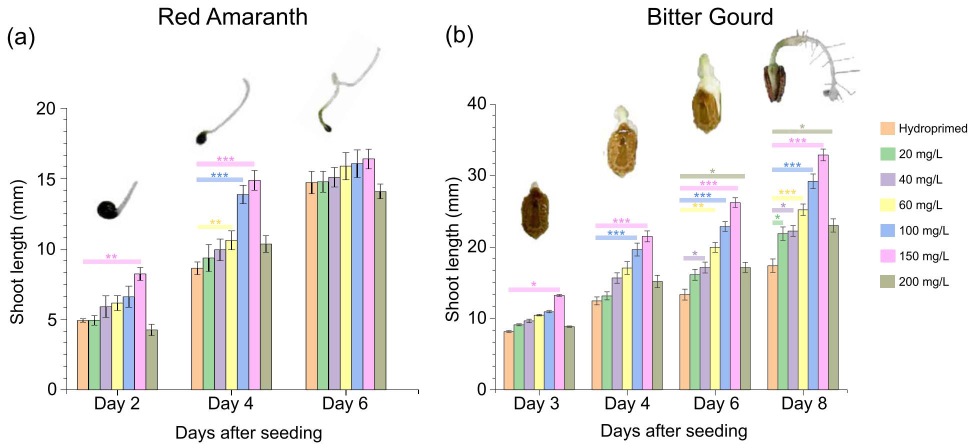

Figure 6. Influence of Type-1 ZnO nanopriming on shoot length dynamics of (a) red amaranth and (b) bitter gourd seedlings. Data are presented as mean ± standard error of the mean based on one set of replication, as no significant differences were found among the triplicates containing 25 seeds each, as determined by ANOVA (see Supplementary Text 6, Tables S4 and S5). Statistical differences between the mean shoot lengths of treatments (various concentrations of ZnO NP priming solutions) compared to the control are denoted by (*, $p < 0.05$; **, $p < 0.01$; ***, $p < 0.001$) according to an independent sample Student's t test.

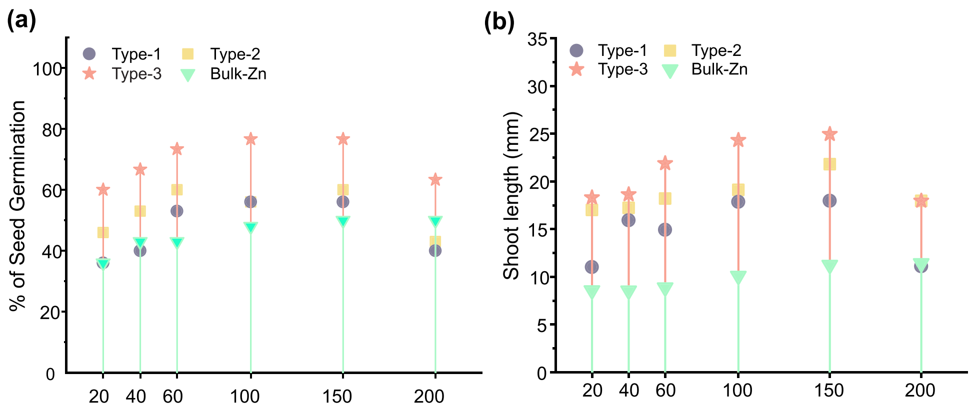

Figure 7. Comparative effect of different NP sizes on (a) seed germination and (b) seedling growth of red amaranth plants on day 6.

such as breaking dormancy, hydrolyzing or metabolizing inhibitors, initiating imbibition, and activating enzymes.[30,56]

Nanoprimed seeds incorporate better seedling growth compared to hydroprimed. In our experiments, we measured the shoot lengths of red amaranth and bitter gourd seedlings. These measurements are conducted alongside germination assessments. We observe a concentration-dependent impact on shoot length, peaking at 150 mg/L. On day 6, we observe enhanced shoot lengths, with a 20% increase in red amaranth and a 40% increase in bitter gourd compared to hydropriming for the 150 mg/L concentration of Type-1 NPs ($p < 0.001$) (Figure 6). A similar trend is observed with Type-2 and Type-3 NPs for both cultivars (Figure S5). This increase is correlated with ZnO NP-mediated factors, acting as nanocatalysts that positively impact the production, transport, and signaling of plant hormones like gibberellins and auxins, crucial for cell division, elongation, and overall seedling growth.[30] Additionally, the unique composition and structure of zinc-rich NPs create oxygen vacancies, triggering a response in plants that stimulates indole acetic acid (IAA) production in root sprouts. Elevated IAA levels promote cell elongation, enhancing shoot development.[55]

The effectiveness of nanopriming in seed germination and seedling growth relies on the concentration of the nanoparticles. In our experiments, higher concentrations, such as 200 mg/L, induce oxidative stress during seed germination, resulting in reduced germination rates for both red amaranth and bitter gourd (Figures 5 and S4). Concurrently, at this concentration, a significant decline in shoot length is consistently observed in both species, emphasizing the detrimental impact of higher nanoparticle concentrations (Figures 6 and S5). This substantial reduction in shoot length indicates that concentrations exceeding a critical threshold adversely affect seedling growth, a phenomenon reported in *Arabidopsis thaliana*[57] and maize,[58] suggesting Zn stress hinders seedling growth. As mentioned above, higher nanoparticle concentrations induce oxidative stress, hindering cell division and elongation, resulting in a marked reduction in shoot length.[59] Additionally, increased ZnO NP concentration leads to the excessive release of Zn^{2+}, disrupting cellular homeostasis, affecting enzymatic activities, and causing dysregulation of specific genes such as ZIP1. This dysregulation impairs the functioning of metal transporters, ultimately resulting in toxic effects on the seedlings.[9,28,60]

Comparative Effects of NP Sizes on Seed Germination and Seedling Growth. The size of the NPs significantly influences their penetration and movement into plant tissues, thereby affecting the effectiveness of nanopriming on seed germination, seedling growth, and plant development. In our study, we conduct seed priming with three distinct sizes of

https://doi.org/10.1021/acsanm.4c00109
ACS Appl. Nano Mater. XXXX, XXX, XXX−XXX

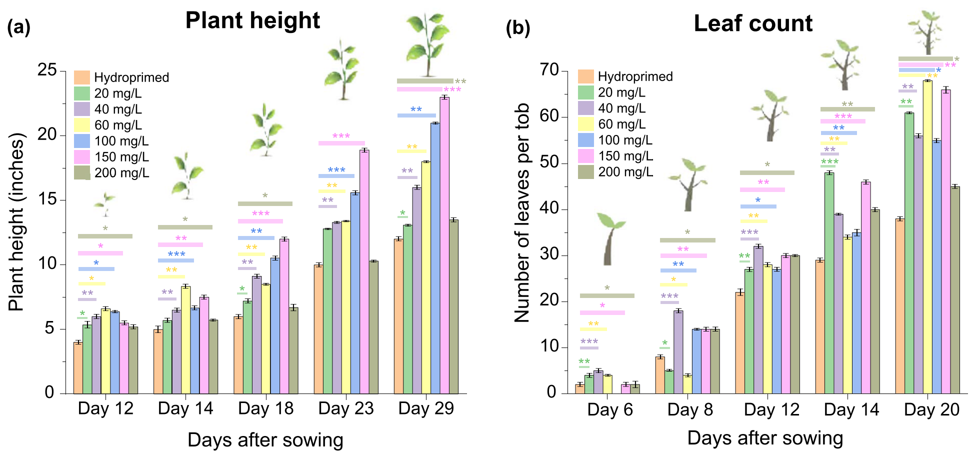

Figure 8. Field study insights: exploring the influence of nanoparticle-mediated seed priming on the growth and development of bitter gourd plants in a real-world setting. (a) Plant height and (b) number of leaves per bed. Data are presented as the mean ± standard error of mean. Statistical differences between treatments (various concentrations of ZnO NP) compared to the control are denoted by (*, $p < 0.05$; **, $p < 0.01$; ***, $p < 0.001$) according to an independent sample Student's t test.

ZnO NPs (∼44 nm, Type-1; ∼ 35 nm, Type-2; ∼ 19 nm, Type-3) alongside bulk $ZnSO_4$ salts (Zn−bulk) primed seeds. Our findings indicate a consistent and gradual improvement in both seed germination and shoot length as the size of NPs decreases, particularly with Type−3 NPs (19 nm) (Figures 7 and S6). Specifically, for red amaranth treated with an optimal concentration of 150 mg/L, Type-3 ZnO NPs show a significant increase of 36, 28, and 53% in FG% compared to Type-1, Type-2, and bulk Zn-treated seeds, respectively (Figure 7a). Regarding shoot length, Type-3 NPs exhibit 39, 14, and 55% enhancement compared to Type−1, Type−2, and bulk−Zn treatments, respectively (Figure 7b). For bitter gourd, Figure S6a indicates no significant effect of NP size variation on FG%. However, for shoot length, Type-3 shows a 45, 23, and 14% enhancement compared to bulk-Zn, Type-1, and Type-2, respectively (Figure S6b). Therefore, our study suggests that the application of the smallest ZnO NPs (Type-3) has a greater impact on seed germination and plant growth than those of Type-1, Type-2, and bulk $ZnSO_4$ salts. This is likely due to the greater capacity of Type−3 to be absorbed and assimilated by the seeds more efficiently, owing to their smallest nanometric size and lowest solubility. This finding aligns with Yusefi et al.'s conclusion that differences in size and morphology contribute to higher growth efficiency.[61]

Plant Fresh Biomass. In our study, we explore the production of fresh biomass as a reliable external indicator, reflecting the internal status of photosynthesis processes within the plant. We directly sow nanoprimed and hydroprimed seeds in plastic pots, simulating field conditions relevant to agricultural production. Our results reveal a positive influence of nanopriming on fresh biomass production, specifically in terms of increased plant height and number of leaves in bitter gourd plants, up to a solution concentration of 150 mg/L compared to the control (see Figure 8). Both our germination and field tests underscore the effectiveness of the 150 mg/L nanopriming concentration in promoting optimal plant growth. At this concentration, there is a significant ($p < 0.001$) increase of 90% in plant height and 74% in the number of leaves compared with hydroprimed plants. The observed increase in the biomass is likely attributed to the crucial role played by Zn ions in ZnO NP-treated seeds. These ions contribute significantly to maintaining the structural integrity of biomembranes by facilitating the accumulation of phospholipids and enhancing protein synthesis within plant cells, as demonstrated in previous research.[62] Additionally, ZnO NPs possess the capability to elevate the overall chlorophyll content in nanoprimed plants. This factor is widely recognized as a pivotal determinant of the plant photosynthetic efficiency. Abdel Latef et al., in their research,[63] suggested that it leads to a significant increase in the overall fresh biomass of the plants.

Biocompatibility of ZnO Nanopriming. Conducting a cytotoxicity study is essential for assessing the potential harm of nanomaterials to living cells and organisms. In investigating the biosafe nature of ZnO NPs, we determine the biocompatibility of ZnO NPs using Hela and Vero cells. The results (Table 1, Figures S7 and 9) show that the synthesized ZnO NPs exhibit biocompatibility at 150 mg/L, with up to 95% cell viability, confirming their nontoxic behavior.

Table 1. Cell Viability Results from the Cytotoxicity Test

sample ID	survival of HeLa cells (%)	survival of Vero cells (%)
solvent (−)	100	100
solvent (+)	>95	>95
Type 1 ZnO NPs	>95	>95
Type 2 ZnO NPs	>95	>95
Type 3 ZnO NPs	>95	>95

Figure S7 presents the photomicrographs of Hela and Vero cells exposed to Type-1 ZnO NPs for 48 h, while Figure 9 illustrates those treated with Type-2 and Type-3 ZnO NPs. By comparing these images with the bulk cells in the control experiments with solvent (−) and solvent (+), it is evident that the cells cultivated with ZnO NPs at a concentration of 150 mg/L exhibit similar shapes and numbers. This resemblance strongly suggests that the ZnO NPs have a benign impact on the cells, preserving their overall characteristics. The data presented in Table 1 summarize the outcomes of the cytotoxicity test.

■ SMART MONITORING SYSTEM

The conventional methods employed for the germination rate and seedling growth monitoring are often manual, labor-

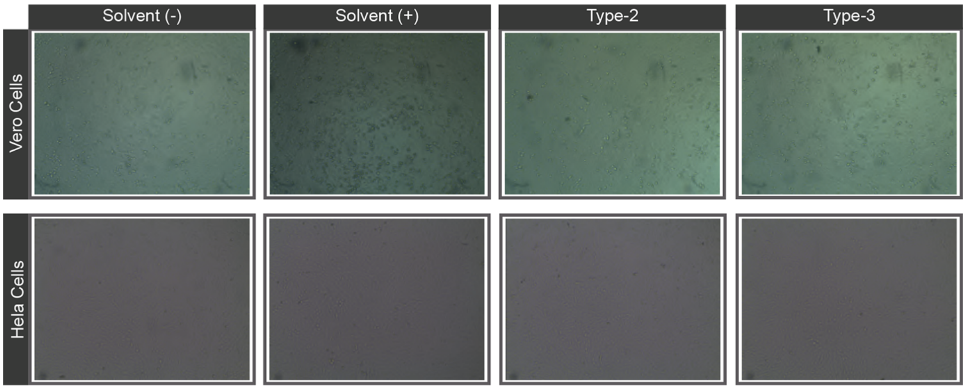

Figure 9. Photomicrographs capture the cellular responses of Hela and Vero cells after a 48 h cultivation with Type-2 and Type-3 ZnO NPs. A comparative analysis with control experiments, showcasing bulk cells in the absence (−) and presence (+) of solvent, indicates a benign impact of the ZnO NPs on the cells.

intensive, and susceptible to inconsistencies. In this paper, we address these challenges by introducing an automated germination detection system based on CNN. However, for field-level system monitoring, a high-throughput solution becomes imperative. To overcome this issue, we present a sophisticated, smart monitoring system. At the core of this system is a custom-designed two-axis CNC machine integrated with a single-board computer and a high-resolution camera. The CNC machine is engineered to capture images of Petri dishes arranged in a standardized three-by-three grid (see Supporting Information Video S1). Maintaining a consistent height for image capture ensures uniformity and high image quality, eliminating common issues, such as the need for image cropping.

The pivotal components of our system include the Raspberry Pi Camera Module V2 paired with a Raspberry Pi V2. This setup accurately captures images of the Petri dishes at predetermined coordinates. Subsequently, these images are automatically uploaded to a designated Google Drive folder, where processing takes place using a CNN running on Google Colab. The CNN is trained to analyze the images, providing precise measurements of the average seed germination rate and seedling growth length. This approach not only streamlines the monitoring process but also yields data that are more accurate and reliable than traditional methods.

■ CONCLUSIONS

In this study, we demonstrate the promising application of nanopriming with ZnO NPs for red amaranth and bitter gourd seeds in the agricultural industry. Our findings reveal that ZnO NPs serve as effective priming agents, accelerating seed germination and seedling growth compared to conventional hydropriming in both cultivars. Through meticulous experimentation and analysis, we identified the optimal priming dose for both species as 150 mg/L, with the smallest NPs (Type-3) yielding the most favorable outcomes. These results underscore the potential of ZnO NPs to enhance the agronomic performance of bitter gourd and red amaranth, ultimately leading to higher yields. Moreover, we have engineered an advanced smart monitoring system that utilizes automation to transform the evaluation of seed germination and growth.

While our current study recommends nanopriming with ZnO NPs as a presowing treatment, further field experimentation is imperative for practical implementation. Moreover, the study suggests a broader exploration of the ZnO NP seed priming across various crop varieties. Plant physiology nuances can influence the interaction with NPs, emphasizing the need for the cautious extrapolation of results from one crop to another. This research not only contributes to the improvement of specific crops but also opens avenues for advancing nanopriming techniques in diverse agricultural contexts.

■ ASSOCIATED CONTENT

Supporting Information

The Supporting Information is available free of charge at https://pubs.acs.org/doi/10.1021/acsanm.4c00109.

Optical studies of ZnO NPs by UV−vis spectrophotometer; compositional analysis of ZnO NPs by FTIR; structural analysis of ZnO NPs by XRD; hydrodynamic size analysis using DLS; elemental composition analysis of soil samples; one-way ANOVA analysis for red amaranth and bitter gourd; Tauc Plots for Type-1,Type-2, and Type-3 ZnO NPs; hydrodynamic size distribution of ZnO NPs; energy-dispersive X-ray spectroscopy (EDX) spectrum illustrating the elemental composition of the soil sample; effect of ZnO NPs priming on the dynamic of Seed germination of red amaranth and bitter gourd; influence of ZnO nanopriming on shoot length dynamics of red amaranth and bitter gourd plants; comparative effect of different NPs sizes on seed gemination, and shoot length of bitter gourd plants; photomicrographs capture the cellular responses of Hela and Vero cells after a 48 h cultivation with Type-1 ZnO NPs; zeta potential and dynamic light scattering for the synthesized ZnO NP at 0.04g/L; photomicrographs capture the cellular responses of Hela and Vero cells after a 48 h cultivation with Type-1 ZnO NPs; zeta potential and dynamic light scattering for the synthesized ZnO NP at 0.04g/L; estimated crystallographic parameters from X-ray diffraction studies; soil elemental analysis for pot cultivation by EDX; p-values obtained from one-way ANOVA between triplicates for red amaranth with Type-1 NPs; p-values obtained from one-way ANOVA between triplicates for bitter gourd with Type-1 NPs; and number of plants in each bed on Day 12 (PDF)

Smart Monitoring System (MOV)

■ AUTHOR INFORMATION

Corresponding Author

Ahsan Habib − *Department of Electrical and Electronic Engineering and Dhaka University Nanotechnology Center, University of Dhaka, Dhaka 1000, Bangladesh;* orcid.org/0000-0003-4636-4718; Email: mahabib@du.ac.bd

Authors

Samia Yeasmin − *Department of Electrical and Electronic Engineering and Semiconductor Technology Research Centre, University of Dhaka, Dhaka 1000, Bangladesh;* orcid.org/0009-0003-5996-3389

Asif Rahman Dipto − *Department of Electrical and Electronic Engineering, University of Dhaka, Dhaka 1000, Bangladesh;* orcid.org/0009-0001-1788-7993

Atique B. Zakir − *Department of Electrical and Electronic Engineering, University of Dhaka, Dhaka 1000, Bangladesh;* orcid.org/0009-0008-2585-0489

Saumik Dey Shovan − *Department of Electrical and Electronic Engineering, University of Dhaka, Dhaka 1000, Bangladesh;* orcid.org/0009-0007-3240-1991

Md Amran Hossen Suvo − *Department of Physics, University of Dhaka, Dhaka 1000, Bangladesh;* orcid.org/0009-0006-8572-7429

Mahabub Alam Bhuiyan − *Semiconductor Technology Research Centre and Department of Physics, University of Dhaka, Dhaka 1000, Bangladesh*

Md. Nurul Amin − *Department of Applied Chemistry and Chemical Engineering, University of Dhaka, Dhaka 1000, Bangladesh;* orcid.org/0000-0003-0070-2611

Taslim Ur Rashid − *Department of Applied Chemistry and Chemical Engineering, University of Dhaka, Dhaka 1000, Bangladesh;* orcid.org/0000-0003-1452-051X

Sharnali Islam − *Department of Electrical and Electronic Engineering and Semiconductor Technology Research Centre, University of Dhaka, Dhaka 1000, Bangladesh;* orcid.org/0000-0002-0218-7337

Complete contact information is available at: https://pubs.acs.org/10.1021/acsanm.4c00109

Notes

The authors declare no competing financial interest.

■ ACKNOWLEDGMENTS

S.I. acknowledges the University Grants Commission of Bangladesh Research Grant 2022-2023. A.H. acknowledges the funding provided by the Collaborative Research Grant from the Faculty of Engineering and Technology at the University of Dhaka and the Special Allocation for Science and Technology 2023−2024 (Project ID: SRG-232417) from the Ministry of Science and Technology, Government of the People's Republic of Bangladesh. The authors extend their sincere thanks for the synthesis facilities provided by the Semiconductor Technology Research Centre (STRC). Gratitude is also due to the Bangladesh Council of Scientific and Industrial Research (BCSIR) for XRD analysis support, and to the Department of Biomedical Engineering at Bangladesh University of Engineering and Technology for facilitating the FESEM studies. The authors appreciate the valuable support from the Food, Nutrition, and Agriculture Laboratory and the Cell and Tissue Culture Laboratory at the Centre for Advanced Research in Sciences (CARS). Finally, thanks are extended to Fab Lab DU and APECE-EEE Alumni Association, University of Dhaka, for their invaluable assistance.

■ REFERENCES

(1) Gilbertson, L. M.; Pourzahedi, L.; Laughton, S.; Gao, X.; Zimmerman, J. B.; Theis, T. L.; Westerhoff, P.; Lowry, G. V. Guiding the design space for nanotechnology to advance sustainable crop production. *Nat. Nanotechnol.* **2020**, *15*, 801−810.

(2) Wang, D.; Saleh, N. B.; Byro, A.; Zepp, R.; Sahle-Demessie, E.; Luxton, T. P.; Ho, K. T.; Burgess, R. M.; Flury, M.; White, J. C.; Su, C. Nano-enabled pesticides for sustainable agriculture and global food security. *Nat. Nanotechnol.* **2022**, *17*, 347−360.

(3) United Nations. *Promoting food security through sustainable agriculture*; UN-iLibrary. 2011

(4) Brodt, S.; Six, J.; Feenstra, G.; Ingels, C.; Campbell, D. Sustainable agriculture. *Nat. Educ. Knowl.* **2011**, *3*, 1.

(5) Kah, M.; Kookana, R. S.; Gogos, A.; Bucheli, T. D. A critical evaluation of nanopesticides and nanofertilizers against their conventional analogues. *Nat. Nanotechnol.* **2018**, *13*, 677−684.

(6) Muhie, S. H. Novel approaches and practices to sustainable agriculture. *Journal of Agriculture and Food Research* **2022**, *10*, No. 100446.

(7) Zhang, P.; Guo, Z.; Ullah, S.; Melagraki, G.; Afantitis, A.; Lynch, I. Nanotechnology and artificial intelligence to enable sustainable and precision agriculture. *Nature Plants* **2021**, *7*, 864−876.

(8) Chariou, P. L.; Dogan, A. B.; Welsh, A. G.; Saidel, G. M.; Baskaran, H.; Steinmetz, N. F. Soil mobility of synthetic and virus-based model nanopesticides. *Nat. Nanotechnol.* **2019**, *14*, 712−718.

(9) Zhao, L.; Bai, T.; Wei, H.; Gardea-Torresdey, J. L.; Keller, A.; White, J. C. Nanobiotechnology-based strategies for enhanced crop stress resilience. *Nature Food* **2022**, *3*, 829−836.

(10) Hofmann, T.; Lowry, G. V.; Ghoshal, S.; Tufenkji, N.; Brambilla, D.; Dutcher, J. R.; Gilbertson, L. M.; Giraldo, J. P.; Kinsella, J. M.; Landry, M. P.; et al. Technology readiness and overcoming barriers to sustainably implement nanotechnology-enabled plant agriculture. *Nat. Food* **2020**, *1*, 416−425.

(11) Lowry, G. V.; Avellan, A.; Gilbertson, L. M. Opportunities and challenges for nanotechnology in the agri-tech revolution. *Nat. Nanotechnol.* **2019**, *14*, 517−522.

(12) Wu, H.; Li, Z. Nano-enabled agriculture: How do nanoparticles cross barriers in plants? *Plant Communications* **2022**, *3*, No. 100346.

(13) Omar, R. A.; Afreen, S.; Talreja, N.; Chauhan, D.; Ashfaq, M. Impact of nanomaterials in plant systems. *Plant nanobionics: Volume 1, advances in the understanding of nanomaterials research and applications* **2019**, 117−140.

(14) Aslani, F.; Bagheri, S.; Muhd Julkapli, N.; Juraimi, A. S.; Hashemi, F. S. G.; Baghdadi, A. Effects of engineered nanomaterials on plants growth: an overview. *Sci. World J.* **2014**, *2014*, No. 641759, DOI: 10.1155/2014/641759.

(15) Singla, R.; Kumari, A.; Yadav, S. K. Impact of nanomaterials on plant physiology and functions. *Nanomaterials and plant potential* **2019**, 349−377.

(16) Adhikary, S.; Biswas, B.; Chakraborty, D.; Timsina, J.; Pal, S.; Chandra Tarafdar, J.; Banerjee, S.; Hossain, A.; Roy, S. Seed priming with selenium and zinc nanoparticles modifies germination, growth, and yield of direct-seeded rice (Oryza sativa L.). *Sci. Rep.* **2022**, *12*, 7103.

(17) Wang, M.; Chen, L.; Chen, S.; Ma, Y. Alleviation of cadmium-induced root growth inhibition in crop seedlings by nanoparticles. *Ecotoxicology and environmental safety* **2012**, *79*, 48−54.

(18) Tripathi, D. K.; Singh, S.; Singh, V. P.; Prasad, S. M.; Dubey, N. K.; Chauhan, D. K. Silicon nanoparticles more effectively alleviated UV-B stress than silicon in wheat (Triticum aestivum) seedlings. *Plant Physiology and Biochemistry* **2017**, *110*, 70−81.

(19) Haydar, M. S.; Ali, S.; Mandal, P.; Roy, D.; Roy, M. N.; Kundu, S.; Kundu, S.; Choudhuri, C. Fe−Mn nanocomposites doped

graphene quantum dots alleviate salt stress of Triticum aestivum through osmolyte accumulation and antioxidant defense. *Sci. Rep.* **2023**, *13*, 11040.

(20) Raza, M. A. S.; Zulfiqar, B.; Iqbal, R.; Muzamil, M. N.; Aslam, M. U.; Muhammad, F.; Amin, J.; Aslam, H. M. U.; Ibrahim, M. A.; Uzair, M. Morpho-physiological and biochemical response of wheat to various treatments of silicon nano-particles under drought stress conditions. *Sci. Rep.* **2023**, *13*, 2700.

(21) Acharya, P.; Jayaprakasha, G. K.; Crosby, K. M.; Jifon, J. L.; Patil, B. S. Nanoparticle-Mediated Seed Priming Improves Germination, Growth, Yield, and Quality of Watermelons (Citrullus lanatus) at multi-locations in Texas. *Sci. Rep.* **2020**, *10*, 5037 DOI: 10.1038/s41598-020-61696-7.

(22) Hong, J.; Wang, C.; Wagner, D. C.; Gardea-Torresdey, J. L.; He, F.; Rico, C. M. Foliar application of nanoparticles: mechanisms of absorption, transfer, and multiple impacts. *Environmental Science: Nano* **2021**, *8*, 1196−1210.

(23) Laware, S.; Raskar, S. Influence of zinc oxide nanoparticles on growth, flowering and seed productivity in onion. *Int. J. Curr. Microbiol. Sci.* **2014**, *3*, 874−881.

(24) Zhang, F.; Yu, J.; Johnston, C. R.; Wang, Y.; Zhu, K.; Lu, F.; Zhang, Z.; Zou, J. Seed priming with polyethylene glycol induces physiological changes in sorghum (Sorghum bicolor L. Moench) seedlings under suboptimal soil moisture environments. *PLoS One* **2015**, *10*, No. e0140620.

(25) Kumar, V. K.; Rajalekshmi, R. Effect of hydro-, halo-and osmopriming on seed germination and seedling performance of Psophocarpus tetragonolobus (L.) DC.(winged bean). *Journal of Crop Science and Biotechnology* **2021**, *24*, 411−428.

(26) Rehman, A.-U.; Fatima, Z.; Qamar, R.; Farukh, F.; Alwahibi, M. S.; Hussain, M. The impact of boron seed priming on seedling establishment, growth, and grain biofortification of mungbean (Vigna radiata L.) in yermosols. *PLoS One* **2022**, *17*, No. e0265956.

(27) Sytar, O.; Kumari, P.; Yadav, S.; Brestic, M.; Rastogi, A. Phytohormone priming: regulator for heavy metal stress in plants. *Journal of Plant Growth Regulation* **2019**, *38*, 739−752.

(28) Savassa, S. M.; Duran, N. M.; Rodrigues, E. S.; de Almeida, E.; van Gestel, C. A. M.; Bompadre, T. F. V.; de Carvalho, H. W. P. Effects of ZnO Nanoparticles on *Phaseolus vulgaris* Germination and Seedling Development Determined by X-ray Spectroscopy. *ACS Appl. Nano Mater.* **2018**, *1*, 6414−6426.

(29) Khepar, V.; Ahuja, R.; Sidhu, A.; Samota, M. K. Nano-sulfides of Fe and Mn Efficiently Augmented the Growth, Antioxidant Defense System, and Metal Assimilation in Rice Seedlings. *ACS Omega* **2023**, *8*, 30231−30238.

(30) Mahakham, W.; Sarmah, A. K.; Maensiri, S.; Theerakulpisut, P. Nanopriming technology for enhancing germination and starch metabolism of aged rice seeds using phytosynthesized silver nanoparticles. *Sci. Rep.* **2017**, *7*, 8263 DOI: 10.1038/s41598-017-08669-5.

(31) Nayeri, S.; Dolatyari, M.; Mouladoost, N.; Nayeri, S.; Zarghami, A.; Mirtagioglu, H.; Rostami, A. Ag/ZnO core−shell NPs boost photosynthesis and growth rate in wheat seedlings under simulated full sun spectrum. *Sci. Rep.* **2023**, *13*, 14385 DOI: 10.1038/s41598-023-41575-7.

(32) Raha, S.; Ahmaruzzaman, M. ZnO nanostructured materials and their potential applications: progress, challenges and perspectives. *Nanoscale Advances* **2022**, *4*, 1868−1925.

(33) Kalimuthu, R.; Sellan, K. M.; Antony, D.; Rajaprakasam, S.; Chokkalingam, V.; Chidambaram, P.; Kanagarajan, S. Nanopriming Action of Microwave-Assisted Biofunctionalized ZnO Nanoparticles to Enhance the Growth under Moisture Stress in *Vigna radiata*. *ACS Omega* **2023**, *8*, 28143−28155.

(34) Kaur, H.; Kaur, H.; Kaur, H.; Srivastava, S. The beneficial roles of trace and ultratrace elements in plants. *Plant Growth Regulation* **2023**, *100*, 219−236.

(35) Verma, S. K.; Das, A. K.; Patel, M. K.; Shah, A.; Kumar, V.; Gantait, S. Engineered nanomaterials for plant growth and development: A perspective analysis. *Science of The Total Environment* **2018**, *630*, 1413−1435.

(36) Kabir, A. H.; Swaraz, A. M.; Stangoulis, J. Zinc-deficiency resistance and biofortification in plants. *J. Plant Nutr. Soil Sci.* **2014**, *177*, 311−319.

(37) Khan, M. N.; Mobin, M.; Abbas, Z. K.; AlMutairi, K. A.; Siddiqui, Z. H. Role of nanomaterials in plants under challenging environments. *Plant Physiology and Biochemistry* **2017**, *110*, 194−209.

(38) Rexlin, J.; Vijayakumar, S.; Nilavukkarasi, M.; Vidhya, E.; Alharthi, N. S.; Sajjad, M.; Punitha, V. N.; Praseetha, P. K. Bioengineered ZnO nanoparticles as a nano priming agent in Cyamopsis tetragonoloba (L). *Taub. to improve yield and disease resistance. Applied Nanoscience* **2023**, *13*, 5993−6001.

(39) Awasthi, A.; Bansal, S.; Jangir, L. K.; Awasthi, G.; Awasthi, K. K.; Awasthi, K. Effect of ZnO nanoparticles on germination of Triticum aestivum seeds. *Macromol. Symp.* **2017**, *376*, No. 1700043, DOI: 10.1002/masy.201700043.

(40) Adhikari, B.; Dhital, P. R.; Ranabhat, S.; Poudel, H. Effect of seed hydro-priming durations on germination and seedling growth of bitter gourd (Momordica charantia). *PloS one* **2021**, *16*, No. e0255258.

(41) Iftikhar, M.; Khan, M. Amaranth. *Bioactive factors and processing technology for cereal foods* **2019**, 217−232.

(42) Qamar, R.; Khan, S.; Safdar, M. E.; Rehman, A.; Javeed, H. M. R.; Nadeem, M. A.; Al-Yahyai, R.; Alkahtani, J. Seed priming with growth regulators modulates production, physiology and antioxidant defense of Indian squash (Praecitrullus fistulosus) under semi-arid conditions. *PLoS One* **2022**, *17*, No. e0265694.

(43) Waqas Mazhar, M.; Ishtiaq, M.; Hussain, I.; Parveen, A.; Hayat Bhatti, K.; Azeem, M.; Thind, S.; Ajaib, M.; Maqbool, M.; Sardar, T.; Muzammil, K.; Nasir, N. Seed nano-priming with Zinc Oxide nanoparticles in rice mitigates drought and enhances agronomic profile. *PLoS One* **2022**, *17*, No. e0264967.

(44) AL-Asady, Z. M.; AL-Hamdani, A. H.; Hussein, M. A. Study the optical and morphology properties of zinc oxide nanoparticles. *AIP Conf. Proc.* **2020**, *2213*, No. 020061, DOI: 10.1063/5.0000259.

(45) Agarwal, S.; Jangir, L. K.; Rathore, K. S.; Kumar, M.; Awasthi, K. Morphology-dependent structural and optical properties of ZnO nanostructures. *Appl. Phys. A: Mater. Sci. Process.* **2019**, *125*, 553 DOI: 10.1007/s00339-019-2852-x.

(46) Iqbal, J.; Abbasi, B. A.; Yaseen, T.; Zahra, S. A.; Shahbaz, A.; Shah, S. A.; Uddin, S.; Ma, X.; Raouf, B.; Kanwal, S.; et al. Green synthesis of zinc oxide nanoparticles using Elaeagnus angustifolia L. leaf extracts and their multiple in vitro biological applications. *Sci. Rep.* **2021**, *11*, 20988.

(47) Sivkov, A. A.; Ivashutenko, A. S.; Rakhmatullin, I. A.; Shanenkova, Y. L.; Osokina, L. V.; Tsimmerman, A. I. Influence of energy parameters on the product of plasmodynamic synthesis of ZnO. *Journal of Physics: Conference Series* **2018**, *1115*, No. 042063.

(48) Kim, K.-M.; Kim, T.-H.; Kim, H.-M.; Kim, H.-J.; Gwak, G.-H.; Paek, S.-M.; Oh, J.-M. Colloidal behaviors of ZnO nanoparticles in various aqueous media. *Toxicology and Environmental Health Sciences* **2012**, *4*, 121−131.

(49) Itroutwar, P. D.; Kasivelu, G.; Raguraman, V.; Malaichamy, K.; Sevathapandian, S. K. Effects of biogenic zinc oxide nanoparticles on seed germination and seedling vigor of maize (Zea mays). *Biocatalysis and Agricultural Biotechnology* **2020**, *29*, No. 101778.

(50) Itroutwar, P. D.; Govindaraju, K.; Tamilselvan, S.; Kannan, M.; Raja, K.; Subramanian, K. S. Seaweed-based biogenic ZnO nanoparticles for improving agro-morphological characteristics of rice (Oryza sativa L.). *Journal of plant growth regulation* **2020**, *39*, 717−728.

(51) David, D. J. Determination of zinc and other elements in plants by atomic-absorption spectroscopy. *Analyst* **1958**, *83*, 655−661.

(52) Robinson, J. W. Atomic absorption spectroscopy. *Anal. Chem.* **1960**, *32*, 17A−29A.

(53) Rai-Kalal, P.; Jajoo, A. Priming with zinc oxide nanoparticles improve germination and photosynthetic performance in wheat. *Plant Physiology and Biochemistry* **2021**, *160*, 341−351.

https://doi.org/10.1021/acsanm.4c00109
ACS Appl. Nano Mater. XXXX, XXX, XXX−XXX

(54) Anand, K. V.; Anugraga, A.; Kannan, M.; Singaravelu, G.; Govindaraju, K. Bio-engineered magnesium oxide nanoparticles as nano-priming agent for enhancing seed germination and seedling vigour of green gram (Vigna radiata L.). *Mater. Lett.* **2020**, *271*, No. 127792.

(55) Prasad, R.; Bhattacharyya, A.; Nguyen, Q. D. Nanotechnology in sustainable agriculture: recent developments, challenges, and perspectives. *Front. Microbiol.* **2017**, *8*, 1014.

(56) Khan, I.; Awan, S. A.; Rizwan, M.; Hassan, Z. U.; Akram, M. A.; Tariq, R.; Brestic, M.; Xie, W. Nanoparticle's uptake and translocation mechanisms in 'plants via seed priming, foliar treatment, and root exposure: A review. *Environmental Science and Pollution Research* **2022**, *29*, 89823−89833.

(57) Nair, P. M. G.; Chung, I. M. Regulation of morphological, molecular and nutrient status in Arabidopsis thaliana seedlings in response to ZnO nanoparticles and Zn ion exposure. *Sci. Total Environ.* **2017**, *575*, 187−198.

(58) Zhang, R.; Zhang, H.; Tu, C.; Hu, X.; Li, L.; Luo, Y.; Christie, P. Phytotoxicity of ZnO nanoparticles and the released Zn (II) ion to corn (Zea mays L.) and cucumber (Cucumis sativus L.) during germination. *Environmental Science and Pollution Research* **2015**, *22*, 11109−11117.

(59) Yin, G.; Xin, X.; Song, C.; Chen, X.; Zhang, J.; Wu, S.; Li, R.; Liu, X.; Lu, X. Activity levels and expression of antioxidant enzymes in the ascorbate−glutathione cycle in artificially aged rice seed. *Plant Physiology and Biochemistry* **2014**, *80*, 1−9.

(60) Kumar, B.; Indu; Singhal, R. K.; Chand, S.; Chauhan, J.; Kumar, V.; Mishra, U. N.; Hidangmayum, A.; Singh, A.; Bose, B.; Kumar, B.; Singhal, R. K.; Chand, S.; Chauhan, J.; Kumar, V.; Mishra, U. N.; Hidangmayum, A.; Singh, A.; Bose, B. Nanopriming in sustainable agriculture: recent advances, emerging challenges and future prospective. In *New and Future Developments in Microbial Biotechnology and Bioengineering*; Elsevier, 2022; pp. 339-365.

(61) Yusefi-Tanha, E.; Fallah, S.; Rostamnejadi, A.; Pokhrel, L. R. Zinc oxide nanoparticles (ZnONPs) as a novel nanofertilizer: Influence on seed yield and antioxidant defense system in soil grown soybean (Glycine max cv. Kowsar). *Sci. Total Environ.* **2020**, *738*, No. 140240.

(62) Yilmaz, A.; Ekiz, H.; Torun, B.; Gultekin, I.; Karanlik, S.; Bagci, S.; Cakmak, I. Effect of different zinc application methods on grain yield and zinc concentration in wheat cultivars grown on zinc-deficient calcareous soils. *Journal of plant nutrition* **1997**, *20*, 461−471.

(63) Abdel Latef, A. A. H.; Abu Alhmad, M. F.; Abdelfattah, K. E. The possible roles of priming with ZnO nanoparticles in mitigation of salinity stress in lupine (Lupinus termis) plants. *Journal of plant growth regulation* **2017**, *36*, 60−70.

https://doi.org/10.1021/acsanm.4c00109
ACS Appl. Nano Mater. XXXX, XXX, XXX−XXX